

Electrical Conductances and association constants in dilute aqueous NdCl_3 solutions from 298 to 523 K along an isobar of 25 MPa

Tae Jun Yoon,^{*} Erica P. Craddock, Katie A. Maerzke, Robert P. Currier, and
Alp T. Findikoglu

Los Alamos National Laboratory, Los Alamos, NM 87545, United States

E-mail: tyoon@lanl.gov

Abstract

Electrical measurements were performed in dilute aqueous NdCl_3 solutions from 298 to 523 K along the 25 MPa isobar to obtain limiting conductances and association constants. The specific conductance data were estimated using a continuous flow cell and a Markov Chain Monte Carlo (MCMC) correction algorithm. The limiting conductances for the salts in water were derived by regressing the mean spherical approximation (MSA) conductance model and speciation analyses based on the MCMC algorithm and the Deep Earth Water (DEW) model. The limiting conductances derived from the experimental data agree well with a predictive correlation proposed by Smolyakov, Anderko, and Lencka. Only the first association constant between neodymium and chloride could be derived at low temperatures (< 373 K) due to the apparent large statistical uncertainty of the second association constant. Above 373 K, both association constants could be derived and show a reasonable agreement with Migdisov and Williams-Jones and Gammons et al.

1 Introduction

Rare earth elements (REEs), a group of elements comprising yttrium, scandium, and lanthanides, are of great importance from an industrial point of view. Their unique physicochemical properties make them essential materials for a variety of state-of-the-art technologies. Neodymium, for instance, is utilized for yttrium aluminum garnet in laser and high-strength permanent magnets. Since the high-strength magnets are used in high-tech electronic and energy technologies, a stable supply chain for these critical materials is necessary for transferring to a carbon-neutral world.

Unfortunately, it is challenging to retrieve REEs in an environmentally benign fashion. Current commercial processes to obtain and refine one ton of REEs discharge 60,000 m³ of waste gas, 2,000 m³ of sewage water, and 1 – 1.4 tons of radioactive waste.¹ Commercial liquid-liquid extraction processes also require up to hundreds of stages of mixers and settlers to separate REEs.² In order to produce REEs in a more environmentally benign manner, various alternative REE resources and techniques are being explored.

Understanding the thermodynamic and kinetic behavior of REEs in natural and artificial systems is required to develop such environmentally-friendly processes.^{3–10} A myriad of theoretical and experimental methods have been adopted to study the thermophysical behavior of aqueous REE solutions. According to previous literature, REEs in an aqueous environment show complicated physicochemical characteristics. For instance, REE chlorides do not form ion aggregates in ambient water, even in modestly concentrated solutions, despite the high valence number (+3) of the REE cations. Bernard et al.¹¹ demonstrated that the equivalent conductances in lanthanum chloride (LaCl₃) solution at room temperature calculated without considering ion pair formation agree with the experimental data. Recent molecular simulations and spectroscopic studies reveal that this non-associating behavior arises from a strong hydration shell.^{6,12} On the other hand, REE sulfates are highly aggregated in an aqueous environment,^{13,14} but their solubilities in water show a retrograde dependence on temperature.

Electrical measurements and analyses in aqueous REE solutions have also been conducted^{14–17} but mainly focused on the solutions at ambient conditions. A recent compilation of literature data by Corti¹⁸ indicates that there is only one study about the experimental measurements of specific conductance in NdCl_3 (*aq*) at elevated temperatures.¹⁹ Ismail et al. measured the specific conductance in dilute rare earth chloride solutions (0.001 mol/kg) from 373 to 673 K along different isobars. They reported that NdCl_3 (*aq*) showed the smallest electrical conductivity among four rare earth chloride solutions and had a conductance maximum at approximately 548 K.

REE solutions at elevated temperatures have been mainly studied based on other theoretical/empirical methods. Using experimental data at 298 K and 1 bar, Haas et al.⁹ proposed thermodynamic parameters for predicting thermodynamic properties of rare earth solutions from 1 to 5,000 bars, and 273 to 1,273 K based on the Deep Earth Water (DEW) model (also known as the extended Helgeson-Kirkham-Flowers model).^{20–25} Gammons et al.²⁶ derived the association constants from solubility experiments and reported that a higher degree of association occurs at high temperatures, compared to the theoretical results proposed by Haas et al.⁹ and Wood et al.²⁷ Migdisov and Williams-Jones²⁸ conducted an ultraviolet spectroscopic study to estimate the association constants. Their results suggest that the first and the second association constants between neodymium and chloride should be lower than Haas et al. at low temperatures, while they become higher at elevated temperatures.

This work aims to obtain the limiting conductance and association constants in dilute aqueous neodymium chloride [NdCl_3 (*aq*)] solutions at elevated temperatures and pressures by measuring and analyzing electrical conductances. A continuous flow cell equipped with an *in-situ* conductometric sensor was utilized to obtain their equivalent conductances at 25 MPa. The conductance data were analyzed based on the Metropolis-Hastings algorithm together with mean spherical approximation (MSA) and chemical speciation analyses proposed in our earlier works.^{29–31}

2 Methods

2.1 Materials

Distilled water (H_2O , Kroger[®]) was purchased in a local store. The specific conductivity of the distilled water was determined as $< 10^{-6}$ S/cm by a handheld conductometer (EW-19601-03, Cole-Parmer[®]). Neodymium chloride hexahydrate ($\text{NdCl} \cdot (\text{H}_2\text{O})_6$, $> 99.0\%$, Sigma Aldrich) was purchased from Sigma Aldrich. No additional purification was performed on the substances.

2.2 Continuous Flow Cell

Feed solutions were prepared using an electronic scale (Model MS 204S/03, Mettler Toledo[®]). Figure 1 shows the schematic of the continuous flow unit. The instrumental details can be found elsewhere.³⁰ Here, only a brief description of the measurement protocol is given. Two high-pressure pumps were used to supply brine solutions from the bottom into a tubular cell. Two thermocouples were used to measure and control the cell temperature. One thermocouple was inserted in the tubular cell to measure the solution temperature directly, while the other measured the cell surface temperature. A split-type heater was used to increase the temperature to the target temperatures. The operating pressure was regulated by a dome-type back pressure regulator connected to a 40 MPa (6,000 psi) argon cylinder. The precision of the pressure transducer installed in this unit was 0.007 MPa (1 psi). A pair of platinized platinum electrodes were inserted into the cell and connected to a frequency response analyzer (Solartron 1260A, Ametek, Inc.). A pair of titanium wires (Ti-6Al-4V, Nexmetal Corporation), which were oxidized at 873 K in air,³² were welded to the electrodes and enveloped in a two-bore alumina rod to immobilize the electrode. The cell was chemically passivated using a citric acid solution to prevent excessive corrosion.³³

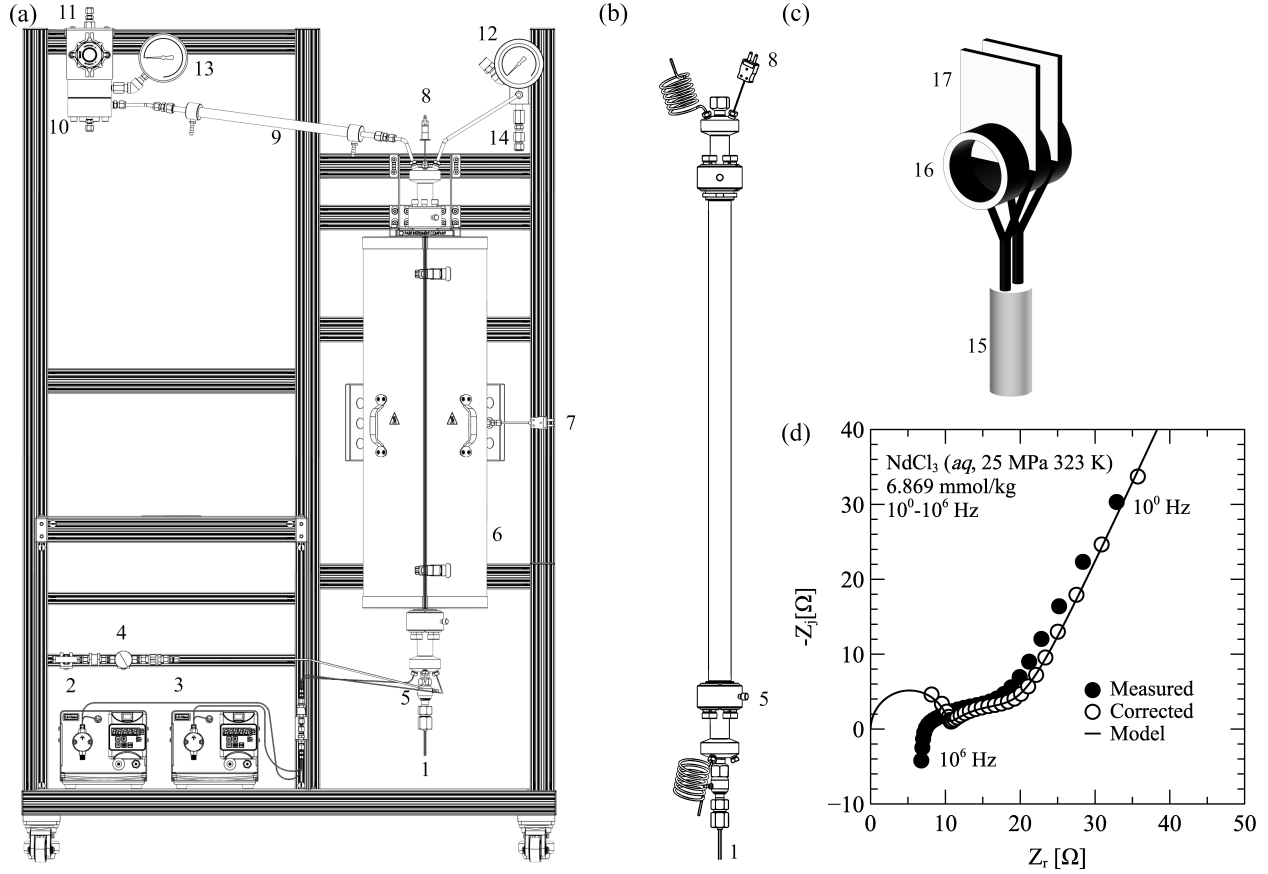


Figure 1: Schematic diagrams of (a) continuous flow unit and (b) vertical flow cell equipped with (c) a pair of in-situ electrodes: 1, electrical feedthrough; 2 and 3, LS-class HPLC pumps; 4, purge line; 5, chiller; 6, split-tube type heater; 7, outside thermocouple; 8, inside thermocouple; 9, single-pass heat exchanger; 10, back pressure regulator; 11, forward pressure regulator (dome); 12, vessel pressure indicator; 13, dome pressure indicator; 14, pressure relief device; 15, two-bore alumina rod; 16, alumina support; 17, platinized platinum plates. Since instrumental artifacts (e.g., wire inductance and parasitic capacitance) influence the impedance spectra, the correction procedure proposed in our earlier works was used to estimate the bulk resistance Z_r and bulk reactance $-Z_i$ in a frequency range from 10^0 to 10^6 Hz as shown in (d).

2.3 Specific Conductance Estimation

We followed the specific conductance estimation protocol suggested in our earlier work for sodium chloride solutions.³⁰ Before every measurement, the cell was flushed with distilled water at elevated temperatures and pressure. After the cell was cooled to 298 K, it was cleaned by supplying additional distilled water at ambient conditions. The cell was dried at 393 K overnight. The *Open* circuit measurement was done before introducing the prepared solutions. The cell was first flushed with one liter of the sample solution to remove any remaining water or corrosion products. Then, it was pressurized to 25 MPa at 298 K and heated to the target temperature(s).

To ensure that (1) no neodymium salt precipitates and (2) no considerable amount of impurities were generated from the cell parts at the target temperatures, an ultraviolet spectrophotometer (Evolution 201, Thermo Scientific, Inc.) was used to analyze the effluent from the continuous flow unit. The ultraviolet calibration curve was constructed by measuring the absorbance of standard neodymium solutions around 574 nm. For the calibration curve, see the Supporting Information in our earlier work.³¹ The specific conductance and the neodymium concentration in the effluent did not show a significant change ($< 2\%$) until the solution temperature reached 523 K. Thus, the *in-situ* specific conductance measurements were performed below 523 K.

When the system temperature read by the inner thermocouple matches the target temperature, the solution impedance ($Z = Z_r + iZ_j$) was measured from 10^0 to 10^6 Hz in triplicate. Here, Z_r and Z_j are real and imaginary parts of the complex impedance, and i is the imaginary unit number $i^2 = -1$. The measured impedance spectra Z_m were averaged and corrected by an *Open/Short* correction algorithm to estimate the impedance of the material under test (MUT). According to the algorithm, the averaged impedance spectrum is given as:

$$Z_m(f) = Z_o(f) + \frac{1}{Z_o^{-1}(f) + Z_{MUT}^{-1}(f)} \quad (1)$$

where Z_O , Z_S , Z_{MUT} are *Open*, *Short*, and *MUT* impedances. By fitting an equivalent circuit model,³⁰ the bulk resistance in a solution (R_{MUT}) was estimated (see Figure 1 (d) and our earlier work³⁰ for the detailed description). The bulk solution resistance was converted to the specific conductance (κ) as:

$$\kappa = \frac{1}{R_{MUT}} \frac{l}{A} \quad (2)$$

where l/A is the cell constant. The cell constant was calculated as $2.985 \pm 0.050 \text{ m}^{-1}$ at room temperature using the specific conductance data provided by Spedding¹⁵ and did not show a noticeable degradation.

2.4 Data Analysis

The specific conductance data estimated from Eq. 2 was converted to equivalent conductance Λ ($\text{S cm}^2/\text{mol}$). It is defined as

$$\Lambda = \frac{\kappa}{N} = \frac{\kappa}{\sum_i^{\text{cations}} c_i z_i} = \frac{\kappa}{\sum_j^{\text{anions}} c_j |z_j|} \quad (3)$$

where N denotes the equivalent concentration (normality, eq/L), and c_k and z_k are the molar concentration and the charge of an ion k . In converting the concentration unit from molality to molarity, it was assumed that the solution density is equal to that of pure water at the same thermodynamic conditions, considering that all solutions are very dilute.^{34,35}

After the pioneering works by Debye and Hückel³⁶ and Onsager,³⁷ a variety of conductance models, including the Shedlovsky model,³⁸ Fuoss-Onsager model,³⁹ Fuoss-Hsia-Fernández-Prini model,⁴⁰ Lee-Wheaton model,^{41–43} Quint-Viallard model,^{44–46} Barthel model (low-concentration chemical model, lcCM),⁴⁷ and mean spherical approximation (MSA) model,^{11,48} were proposed. In the field of high-temperature and high-pressure aqueous chemistry, the Turq-Blum-Bernard-Kunz (TBBK) model⁴⁸ and the Fuoss-Hsia-Fernández-Prini (FHFP) model⁴⁰ have been widely used. Since the FHFP model is suitable only for symmetric electrolytes, the TBBK model was adopted in this work.

The TBBK model calculates the equivalent conductance based on the MSA theory. The equivalent conductance contribution of a single species k (λ_k) is given as:

$$\lambda_k = \lambda_k^\infty \left(1 + \frac{\delta v_k}{v_k} \right) \left(1 + \frac{\delta X}{X} \right) \quad (4)$$

where λ_k^∞ is the limiting conductance of the species k , $\delta v_k/v_k$ is the electrophoretic contribution, and $\delta X/X$ is the relaxation contribution, including the hydrodynamic term. Each term is a complex function of the size parameter σ_k , concentration c_k , static permittivity ϵ_r , and solvent viscosity η . See Supporting Information for all expressions (all known misprints^{49,50} in the original article by Turq et al.⁴⁸ were corrected). Static permittivity and viscosity of pure water were calculated from Fernández et al.⁵¹ and Huber et al.⁵² The solution densities were assumed to be equal to the solvent densities calculated from the Wagner-Pruß equation of state.⁵³

The limiting conductance λ_k^∞ of the species k is defined as

$$\lambda_k^\infty = \lim_{c_k \rightarrow 0} \lambda_k(c_k) \quad (5)$$

where c_k is the molar concentration of the species k . It is directly related to the limiting diffusion coefficient of the species k (D_k^∞) as:^{48,54,55}

$$\frac{D_k^\infty}{\lambda_k^\infty} = \frac{RT}{z_k F^2} \quad (6)$$

where R is the universal gas constant, z_k is the charge, and F is the Faraday constant.

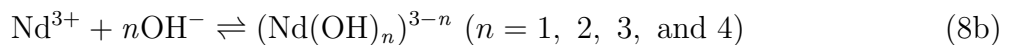
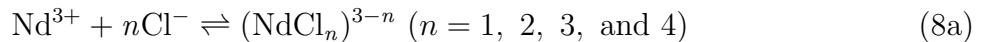
Although the TBBK model has been widely utilized, several inconsistencies were reported between the model predictions and the empirical results. Thus, the original TBBK model was modified following the suggestions in earlier studies.^{49,50,56–58} First, the Bjerrum distance between cation and anion pairs was used as the size parameter for calculating the electrostatic part of the activity coefficient y_i in the MSA formalism.⁵⁰ Second, the first-order mixing rule

proposed by several authors⁵⁶⁻⁵⁹ and tested by Sharygin et al.⁵⁰ was adopted to calculate the equivalent conductance, considering ion-pair formation in the system. This procedure was essential since neodymium ion is poly-valent and forms hydroxide complexes $\text{Nd}(\text{OH})_n$ shifting the acid-base equilibrium in the system.⁹ The mixing rule is given as:

$$\Lambda = \sum_i^{\text{cations}} \sum_j^{\text{anions}} f_i f_j l_{ij}(\Gamma) \quad (7)$$

where the sum is over all cation-anion pairs (i, j) in the system. The normalized fraction of a species k (f_k) is defined as $f_k \equiv c_k |z_k| / N$, and the pair equivalent conductance contribution $l_{ij}(\Gamma)$ is calculated based on the original TBBK equations given in the Supporting Information. Note that the screening parameter Γ was calculated by considering not just a single pair (i, j) , but all species in the system.⁶⁰

The ion pairs and free ions concentrations were calculated using the ion speciation algorithm developed in our earlier work.³¹ In this algorithm, chemical equilibria between different species should be first determined. In NdCl_3 solutions, the following equilibria can be considered.



We neglected the third and fourth chemical equilibria between Nd^{3+} and Cl^- , considering their population is much lower than the other species; the association constants cannot be estimated reliably. Unlike neutral salts like sodium chloride, the neodymium ion forms a pair with hydroxide ion(s) $\text{Nd}(\text{OH})_n$. The formation of neodymium hydroxide complexes increases the hydrogen ion concentration, which could significantly contribute to the total equivalent conductance. Thus, the neodymium-hydroxide equilibria were always included. The Bandura-Lvov equation was used to calculate the self-ionization constant.⁶¹ The activity

coefficients y_i 's were calculated by using the modified protocol suggested by Sharygin et al.⁵⁰ (see the Supporting Information for the detailed calculation procedure).

After calculating the association constants and activity coefficients, the whole set of equations, including the mass and charge balance (electroneutrality) equations, were solved simultaneously using the modified Powell method.

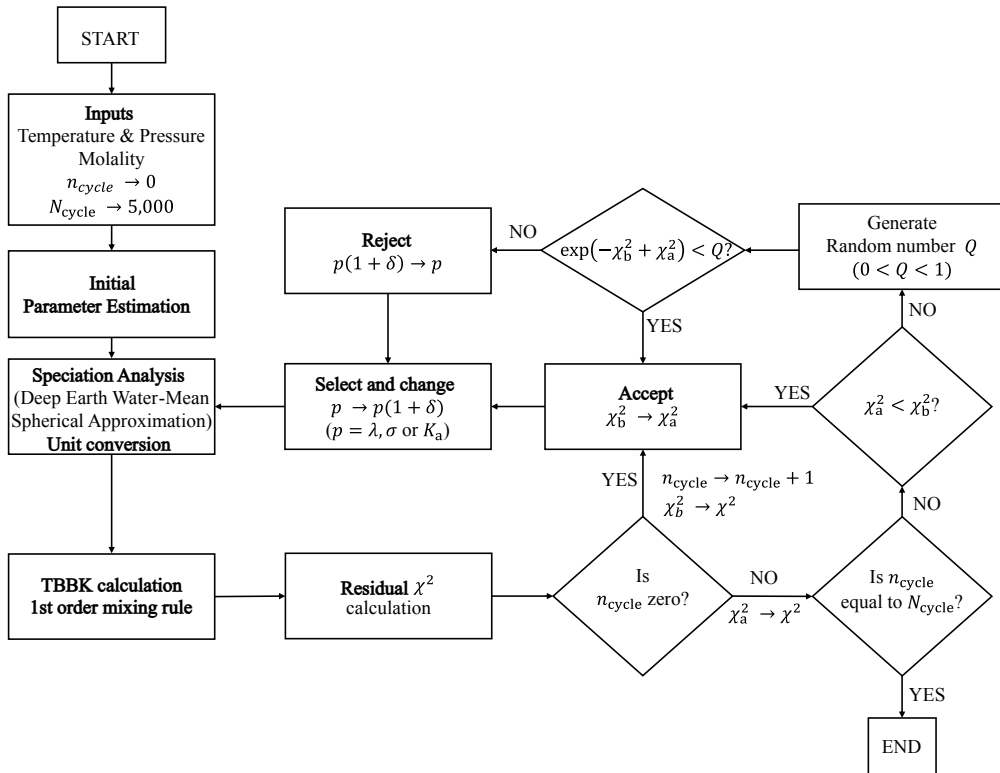


Figure 2: A model regression algorithm based on the Metropolis-Hastings (Markov Chain Monte Carlo) algorithm. For calculation details (parameter initialization, Turq-Blum-Bernard-Kunz equation calculation, and first order mixing rule), see the main text and the Supporting Information.

Assembling all addressed points, an iterative procedure was designed to regress the TBBK equation to the experimental data (Figure 2), which is similar to that proposed by Zimmerman,⁶² except that the solution density is assumed to be equal to the solvent density and the Metropolis-Hastings algorithm is used for model regression. In this procedure, the limiting conductance λ_k^∞ and size parameters are first estimated. The limiting conductance of Cl^- is estimated using an empirical correlation recently proposed by Zimmerman, Arcis, and

Tremanne.⁶³ It is given as:

$$\lambda_{\text{Cl}}^{\infty} = A_1 \eta^{A_2 + A_3 / \rho_w} \quad (9)$$

where A_1 , A_2 , and A_3 are adjustable parameters ($A_1 = 1.137 \pm 0.006$, $A_2 = -0.925 \pm 0.002$, and $A_3 = 34.44 \pm 1.24$), η is the solvent viscosity in Poise, and ρ_w is the solvent density in kg/m^3 . The limiting conductivities of hydrogen and hydroxide ions (λ_{H} and λ_{OH}) were calculated from an empirical correlation proposed by Marshall.⁶⁴ The limiting conductivity of Nd^{3+} ($\lambda_{\text{Nd}}^{\infty}$) was assigned arbitrarily.

The crystallographic radii taken from Marcus⁶⁵ were mainly used to fit the experimental data except those at 298 K (see Sec. 3.1). The first and the second association constants between Nd and Cl ions (K_{NdCl} and K_{NdCl_2}) were initially estimated using the DEWPython module.²⁵ The DEW parameters provided by Migdisov and Williams-Jones²⁸ and those by Haas et al.⁹ were used as initial estimates of K_{NdCl} and K_{NdCl_2} . The converged values with different initial association constants were not significantly different. The other association constants for neodymium and hydroxide ions were calculated based on the DEW parameters proposed by Haas et al.⁹ and were not altered in the fitting procedure.

The limiting conductance and the size parameter of an ion pair P consisting of the m number of ions were estimated as:

$$\lambda_{\text{P}}^{\infty} = \frac{|z_{\text{P}}|}{\left(\sum_{i=1}^m (z_i / \lambda_i^{\infty})^3\right)^{1/3}} \quad (10a)$$

$$\sigma_{\text{P}} = \left(\sum_{i=1}^m \sigma_i^3\right)^{1/3} \quad (10b)$$

After the initialization, the limiting conductivity of the neodymium ion $\lambda_{\text{Nd}}^{\infty}$ and the association constants K_{NdCl} and K_{NdCl_2} were changed based on the Metropolis-Hastings algorithm.²⁹ In this algorithm, one of the adjustable parameters p is randomly chosen and changed to $p' = p(1 + \delta)$, where δ is a random number between $-M$ and M . The magnitude M was 0.05 in this work. When N_{p} data points are given, the residual between the model

calculation and the experimental data is evaluated as:

$$\chi^2 = \sum_{i=1}^{N_P} (\Lambda_i^{\text{calc}} - \Lambda_i^{\text{meas}})^2 \quad (11)$$

where Λ_i^{calc} and Λ_i^{meas} are the calculation results and experimental data point at the i^{th} point. When the residual calculated from the changed parameters is lower than that from the original parameters, the changed parameter p' is accepted. If not, a random number between zero and one is generated, and compared to $\exp(-\chi_{\text{after}}^2 + \chi_{\text{before}}^2)$. If the random number is smaller than $\exp(-\chi_{\text{after}}^2 + \chi_{\text{before}}^2)$, the result is accepted. Otherwise, the result is rejected. This procedure is repeated until all parameters are converged. In fitting the model to the equivalent conductance data, the second association constant K_{NdCl_2} did not show a stable convergence at low temperatures. It showed a variation from 10^{-7} to 10. This result suggests that K_{NdCl_2} has no significant contribution to the conductance data. (see Sec. 3) In this case, only the first association step was considered in the fitting procedure.

After the fitting procedure, the discrepancy between the model and the experimental data was evaluated using absolute average relative deviation (AAD). It is defined as:

$$\text{AAD} = \left(\frac{|\Lambda^{\text{calc}} - \Lambda^{\text{meas}}|}{\Lambda^{\text{meas}}} \right) 100 \text{ [\%]} \quad (12)$$

3 Results and discussion

3.1 Model validation

Before analyzing the experimental data obtained in this work, we attempted to fit the TBBK model to literature data taken from Spedding and coworkers.^{15,16} (Figure 3) The fitting concentration range was limited to $c \leq 1$ mol/L, considering the model limitation proposed by Turq et al.⁴⁸ The model calculation results did not change significantly when the ion pair formation between neodymium and chloride ions was neglected. Instead, the deviation

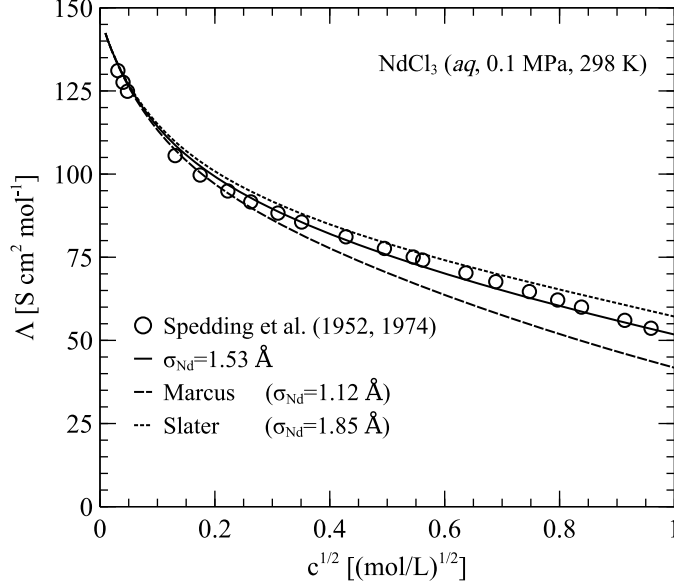


Figure 3: TBBK model fit to the equivalent conductance data in NdCl_3 (*aq*) measured by Spedding and coworkers at 298 K and 1 bar. The fitting result was not significantly influenced by the ion pair formation between chloride and neodymium. Rather, the goodness of fit was affected by the size parameter of the neodymium ion.

between the model and the empirical data depended on the size parameter σ_{Nd} . When the crystallographic radius taken from Marcus was used ($\sigma_{\text{Nd}} = 1.12 \text{ \AA}$), the predicted conductance was close to the experimental data in dilute solutions ($c^{1/2} < 0.25(\text{mol/L})^{1/2}$, AAD 1.246 %) but became lower than the experimental data in concentrated solutions (overall AAD 8.29 %). When the Slater radius⁶⁶ ($\sigma_{\text{Nd}} = 1.85 \text{ \AA}$) was used, the model over-predicted the conductance within the fitting concentration range (AAD 3.85 %). By fixing the limiting conductance of the neodymium ion to be $69.8 \text{ S cm}^2/\text{mol}$,^{16,17} the optimal ionic radius to fit the experimental data within $c < 1.0 \text{ mol/L}$ was obtained as 1.53 \AA with an overall AAD of 1.93 %. When only dilute solutions were fitted, the optimal radius became close to the crystallographic radius $\sigma_{\text{Nd}} = 1.12 \text{ \AA}$. The dependence of the optimal radius on the ionic strength of the system may indicate that a rigid hydration shell is formed in NdCl_3 (*aq*).^{6,12} Since this work only focuses on dilute solutions at elevated temperatures, we used the crystallographic radius throughout.⁶⁵

It is noteworthy that the above results are not sensitive to the association constants.

That is, the calculation results do not vary significantly depending on the association constants. Moreover, the results show a similar behavior without considering the association. The insensitivity of the conductance data to small association constants does not arise from the deficiency in the TBBK model. Indeed, rare earth chlorides in water at room temperature are sometimes regarded as non-associating solutes. For instance, Apelblat¹⁷ used the Quint-Viallard model^{44–46} for dilute NdCl_3 solutions at 298 K without considering the ion association. Bernard et al.¹¹ demonstrate that the non-associative model can predict the equivalent conductances in lanthanum chloride solutions up to 1 mol/L. Thus, the insensitivity of the conductance data to association constants may indicate the limit of the conductance method to calculate the association constants in weakly associating electrolyte solutions.⁴⁹ The statistical uncertainty of the second association constants was also large at low temperatures studied in this work. (Sec. 3.2)

3.2 Model regression

Table 1: Specific conductance (κ_{meas}) and equivalent conductance (λ_{meas}) data and the TBBK model regression results (λ_{calc}) at different temperatures and concentrations along an isobar of 25 MPa. The unit eq/L indicates equivalent molarity.

$m \times 10^3$	$N \times 10^3$	κ_{meas}	λ_{meas}	λ_{calc}	AAD
[mol/kg]	[eq/L]	[$\mu\text{S cm}^{-1}$]	[$\text{S cm}^2 \text{ mol}^{-1}$]	[$\text{S cm}^2 \text{ mol}^{-1}$]	[%]
$T = 323 \text{ K}, p = 25 \text{ MPa}, \rho_w = 998.7 \text{ kg/m}^3$					
0.371	1.111	240.1	216.1 ± 1.6	215.9	0.10
0.767	2.297	483.1	210.3 ± 2.3	209.8	0.22
1.516	4.540	919.8	202.6 ± 0.9	202.8	0.11
2.815	8.428	1654.8	196.3 ± 1.5	195.2	0.61
3.989	11.939	2277.1	190.7 ± 0.3	190.3	0.23
5.444	16.287	3032.8	186.2 ± 0.6	185.6	0.32

Continued on next page

$m \times 10^3$	$N \times 10^3$	κ_{meas}	λ_{meas}	λ_{calc}	AAD
[mol/kg]	[eq/L]	$[\mu\text{S cm}^{-1}]$	$[\text{S cm}^2 \text{ mol}^{-1}]$	$[\text{S cm}^2 \text{ mol}^{-1}]$	[%]
6.869	20.543	3702.7	180.2 ± 0.4	181.9	0.94
$T = 348 \text{ K}, p = 25 \text{ MPa}, \rho_w = 985.7 \text{ kg/m}^3$					
0.371	1.097	333.5	304.1 ± 1.1	305.1	0.32
0.767	2.267	669.6	296.3 ± 0.6	295.3	0.32
1.516	4.481	1274.5	287.0 ± 1.0	284.4	0.91
2.815	8.318	2269.5	275.6 ± 0.7	272.8	0.99
3.989	11.784	3129.5	266.8 ± 1.2	265.6	0.44
5.444	16.075	4158.7	259.4 ± 0.9	258.7	0.27
6.869	20.276	5191.3	256.0 ± 0.8	253.3	1.06
$T = 373 \text{ K}, p = 25 \text{ MPa}, \rho_w = 969.7 \text{ kg/m}^3$					
0.371	1.079	436.8	404.8 ± 1.3	404.2	0.15
0.767	2.231	872.9	391.3 ± 2.3	389.8	0.38
1.516	4.409	1650.2	374.3 ± 1.3	374.4	0.03
2.815	8.184	2931.4	358.2 ± 0.9	358.5	0.08
3.989	11.594	4052.1	349.5 ± 0.8	348.6	0.25
5.444	15.816	5348.5	338.2 ± 0.4	339.4	0.36
6.869	19.950	6598.1	330.7 ± 1.2	332.1	0.43
$T = 398 \text{ K}, p = 25.0 \text{ MPa}, \rho_w = 951.3 \text{ kg/m}^3$					
0.371	1.058	539.0	509.3 ± 1.1	508.7	0.12
0.767	2.188	1063.1	485.8 ± 2.9	487.4	0.31
1.516	4.325	2003.9	463.4 ± 2.7	465.2	0.41
2.815	8.028	3537.4	440.6 ± 3.7	443.1	0.57
3.989	11.373	4879.2	429.0 ± 2.7	429.8	0.19
5.444	15.515	6407.3	413.0 ± 2.1	417.5	1.09

Continued on next page

$m \times 10^3$	$N \times 10^3$	κ_{meas}	λ_{meas}	λ_{calc}	AAD
[mol/kg]	[eq/L]	$[\mu\text{S cm}^{-1}]$	$[\text{S cm}^2 \text{ mol}^{-1}]$	$[\text{S cm}^2 \text{ mol}^{-1}]$	[%]
6.869	19.570	7907.6	404.1 ± 0.2	408.0	0.96
$T = 423 \text{ K}, p = 25.0 \text{ MPa}, \rho_w = 930.4 \text{ kg/m}^3$					
0.371	1.035	635.8	614.2 ± 2.5	614.8	0.09
0.767	2.140	1245.1	581.7 ± 1.6	584.6	0.49
1.516	4.230	2331.1	551.1 ± 1.3	553.4	0.42
2.815	7.852	4081.8	519.8 ± 1.2	522.9	0.60
3.989	11.124	5606.0	504.0 ± 1.9	505.0	0.21
5.444	15.176	7419.7	488.9 ± 3.4	488.7	0.03
6.869	19.142	9112.5	476.0 ± 0.5	476.4	0.07
$T = 448 \text{ K}, p = 25.0 \text{ MPa}, \rho_w = 907.2 \text{ kg/m}^3$					
0.371	1.009	723.1	716.4 ± 1.7	715.0	0.19
0.767	2.087	1399.7	670.7 ± 1.1	674.8	0.61
1.516	4.125	2593.5	628.8 ± 1.1	631.4	0.41
2.815	7.657	4496.7	587.3 ± 3.6	589.4	0.36
3.989	10.847	6115.0	563.8 ± 1.3	565.3	0.28
5.444	14.798	8028.2	542.5 ± 3.3	543.8	0.23
6.869	18.666	9835.6	526.9 ± 0.2	527.6	0.13
$T = 473 \text{ K}, p = 25.0 \text{ MPa}, \rho_w = 881.5 \text{ kg/m}^3$					
0.371	0.981	787.5	802.9 ± 3.4	800.7	0.28
0.767	2.028	1520.5	749.9 ± 3.2	748.2	0.22
1.516	4.008	2714.3	677.3 ± 4.6	687.5	1.51
2.815	7.440	4672.1	628.0 ± 0.7	629.2	0.20
3.989	10.540	6295.2	597.3 ± 1.1	596.8	0.08
5.444	14.379	8207.6	570.8 ± 1.3	568.5	0.41

Continued on next page

$m \times 10^3$	$N \times 10^3$	κ_{meas}	λ_{meas}	λ_{calc}	AAD
[mol/kg]	[eq/L]	$[\mu\text{S cm}^{-1}]$	$[\text{S cm}^2 \text{ mol}^{-1}]$	$[\text{S cm}^2 \text{ mol}^{-1}]$	[%]
6.869	18.138	9949.0	548.5 ± 1.4	547.6	0.17
$T = 498 \text{ K}, p = 25 \text{ MPa}, \rho_w = 853.0 \text{ kg/m}^3$					
0.371	0.949	832.0	876.7 ± 8.9	869.5	0.83
0.767	1.962	1579.8	805.2 ± 2.5	799.7	0.68
1.516	3.878	2744.7	707.8 ± 3.2	714.8	1.00
2.815	7.199	4671.9	649.0 ± 1.5	634.9	2.17
3.989	10.199	6012.2	589.5 ± 0.9	592.1	0.44
5.444	13.914	7769.7	558.4 ± 2.8	555.7	0.48
6.869	17.552	9568.3	545.1 ± 1.7	529.6	2.86
$T = 523 \text{ K}, p = 25 \text{ MPa}, \rho_w = 821.1 \text{ kg/m}^3$					
0.371	0.914	852.3	932.9 ± 7.7	930.1	0.31
0.767	1.889	1602.3	848.3 ± 1.7	842.5	0.69
1.516	3.733	2727.6	730.6 ± 0.2	732.1	0.20
2.815	6.931	4355.9	628.5 ± 2.6	629.5	0.16
3.989	9.819	5703.8	580.9 ± 0.4	575.9	0.86
5.444	13.396	7151.3	533.8 ± 1.5	531.3	0.48
6.869	16.898	8658.7	512.4 ± 0.6	499.6	2.49

Figure ?? (a) shows the specific conductance data estimated from the measured impedance spectra. All specific conductance data show an almost linear increase at $T < 425 \text{ K}$ due to the increase in kinetic energy of individual ions and the increase in the hydrogen ion concentration. Above 425 K, the specific conductance curves become concave downward. At concentrations below 1.516 mmol/kg, no conductance maximum was observed. The specific conductance maximum is observed as the concentration increases and shifts to a lower temperature ($\sim 473 \text{ K}$). This result would arise from ion pair formation, as demonstrated

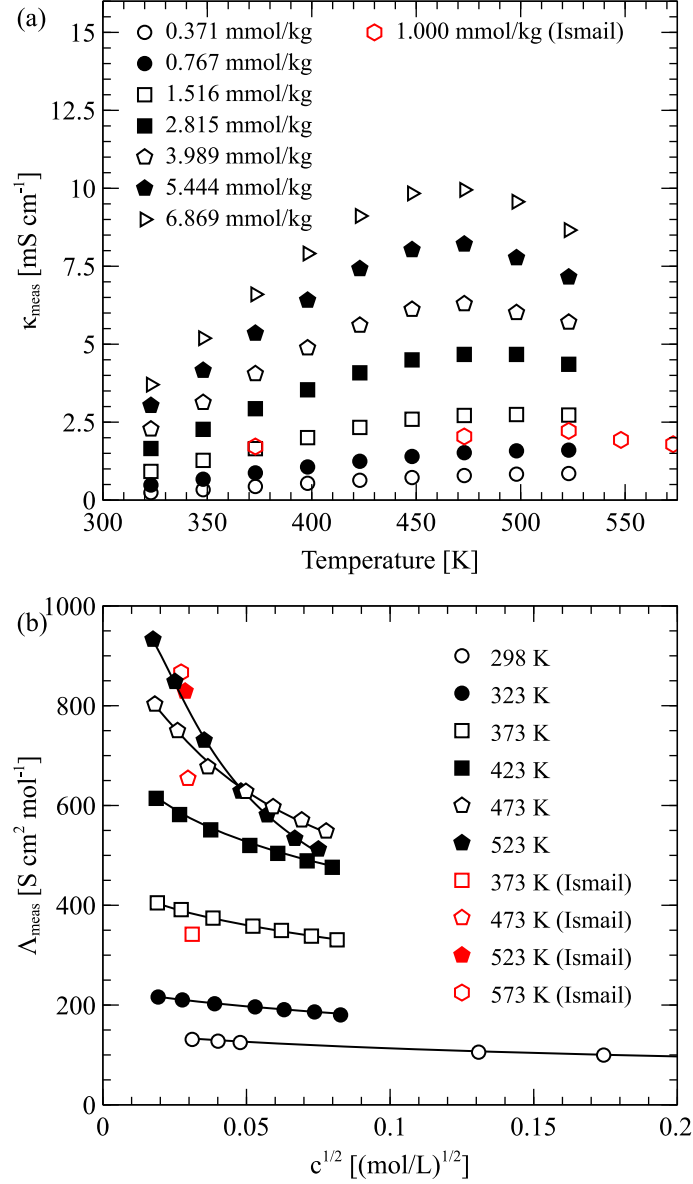


Figure 4: (a) Specific conductance estimated from the impedance spectra. (b) Equivalent conductance data (symbols) and the TBBK fitting results (lines). In (b), the data were represented with a 50 K interval for visual clarity (except the literature data by Spedding et al.^{15,16}) Red symbols were calculated from the experimental data measured by Ismail et al. (24.52 MPa, $m = 1.00$ mmol/kg)¹⁹ They show a reasonable agreement with our data (AAD < 10%).

in our earlier simulation work on NaCl.⁶⁷ Considering that (1) 1 mmol/kg NdCl₃ (*aq*) has a conductance maximum at ~ 548 K¹⁹ and (2) the specific conductance data obtained by Ismail et al.¹⁹ shows a reasonable agreement with ours, the measured specific conductance data seem reliable.

Figure ?? (b) shows the equivalent conductance data and the TBBK model regression results. The equivalent conductance data from 323 to 523 K are presented with a 50 K interval for visual clarity (see Table 1 for the equivalent conductance data estimated at other temperatures). The average AAD between the model and the experimental data was 0.5 %. At low temperatures, the equivalent conductance shows a linear dependence on the square root of the concentrations ($c^{1/2}$), following the limiting law (Debye-Hückel-Onsager equation). As the temperature increases, the equivalent conductance curve along an isotherm becomes concave upwards, implying ion pair formation. The equivalent conductance data at 24.52 MPa measured by Ismail et al.¹⁹ was obtained by converting the specific conductances to the equivalent conductances as follows. Since Ismail et al. prepared stock solution(s) of 0.997 mM solution at room temperature, the density polynomial proposed by Spedding et al.¹⁵ was used to convert the concentration unit from molarity to molality at room temperature, and normality at different conditions were calculated based on the solvent densities calculated from Wagner-Pruß equation.⁵³ The converted data show a reasonable agreement with our data; AAD at similar thermodynamic conditions is below 10 %).

Table 2 shows the limiting conductance data obtained by fitting the TBBK equation. We compared the limiting conductance from the conductometric measurements to the Smolyakov-Anderko-Lencka correlation.^{58,68} It is given as:

$$\ln \lambda_i^\infty(T) = A + B/T \quad (13)$$

where A and B are adjustable parameters. Anderko and Lencka proposed a correlation between the structural entropy ΔS_{str}^0 , a structural component of the hydration entropy,⁶⁹

and the adjustable parameter B . Based on this correlation and the limiting conductance of Nd^{3+} at 298 K, the predictive equation [Eq. 13] was used to calculate $\lambda_{\text{Nd}}^{\infty}$. The limiting conductances experimentally estimated from our data are consistent with those from the Smolyakov-Anderko-Lencka correlation. (Figure 5)

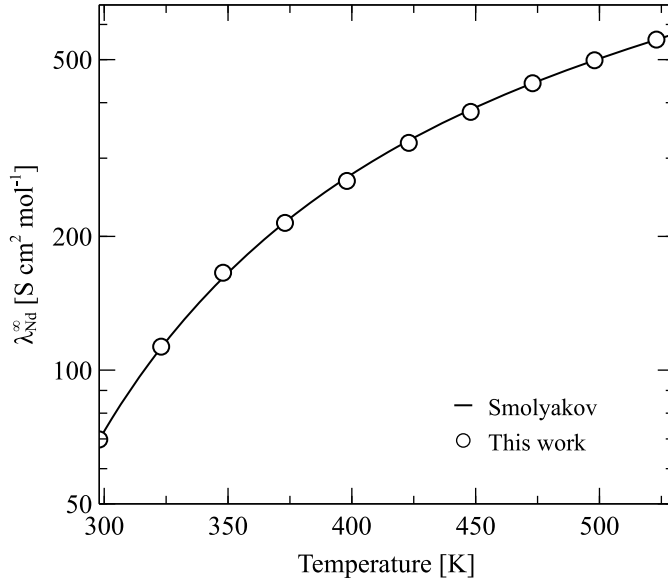


Figure 5: Comparison between the limiting conductances regressed from the TBBK model (open circles) and those from the Anderko-Lencka-Smolyakov equation (solid line). They agree well with each other.

Note that the Smolyakov equation is similar to the correlation proposed by Zimmerman, Arcis, and Tremaine (Eq. 9). When Eq. 9 was fitted, the fitting parameters were obtained as $A_1 = 0.67$, $A_2 = -0.97$ and $A_3 = -13.97$ (AAD 0.69 %).

Using the Smolyakov-Anderko-Lencka equation, the specific conductance data were generated based on different association constant models proposed by Haas et al.⁹ and Migidsov and Williams-Jones.²⁸ Figure 6 compares the calculated specific conductance data to the measured ones. Although the second association constants are different by up to a factor of $\mathcal{O}(10^2)$, the specific conductance difference between these two models is comparable to the measurement uncertainties at low temperatures. This result suggests that the second association constants at low temperatures cannot be reliably derived. Indeed, when both the first and the second association steps are considered in model regression at low temper-

Table 2: Limiting conductances of the neodymium ion from 298 to 523 K along an isobar of 25 MPa.

T [K]	$\lambda_{\text{Nd}}^{\infty}$ (TBBK) [$\text{S cm}^2 \text{mol}^{-1}$]	$\lambda_{\text{Nd}}^{\infty}$ (Eq. 13) [$\text{S cm}^2 \text{mol}^{-1}$]
298	69.8 ^a	70.0
323	112.9 ± 3.0	112.6
348	165.7 ± 2.6	161.8
373	214.5 ± 1.1	215.5
398	266.6 ± 1.7	271.9
423	324.8 ± 2.3	329.2
448	381.4 ± 3.4	386.3
473	442.4 ± 7.7	442.7
498	498.4 ± 16.2	498.7
523	554.7 ± 20.3	555.0

^a0.1 MPa data from Apelblat¹⁷ and Spedding et al.¹⁵

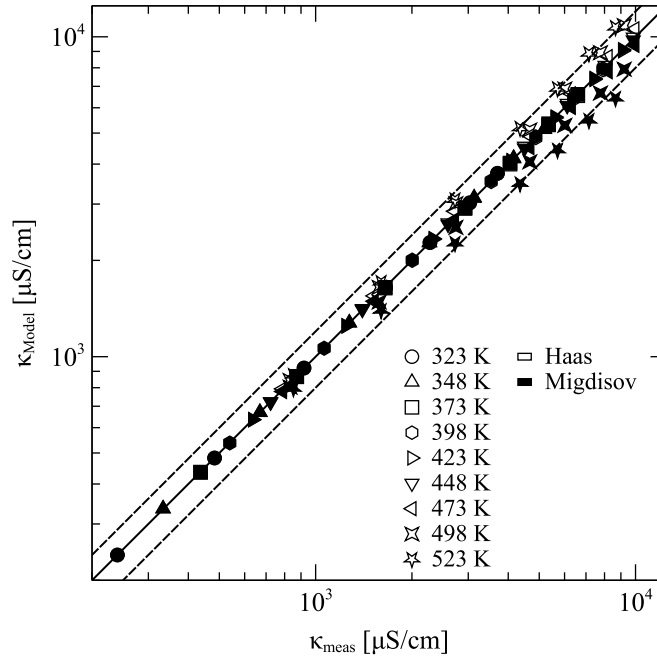


Figure 6: A parity plot between the specific conductance data obtained from this work and those calculated based on the association constants by Haas et al.⁹ (open symbols) and Migdisov and Williams-Jones²⁸ (filled symbols). At low temperatures, the empirical data and those calculated from two different models agree well with each other even when the association constants are different by a factor of $\mathcal{O}(10^2)$. At higher temperatures (> 398 K), the measured conductance becomes higher than those calculated using the DEW parameters by Migdisov and Williams-Jones²⁸ but lower than those from Haas et al.⁹ The dashed lines represent AAD ± 15 % lines. For numerical details, see the Table S3 in Supporting Information.

atures, the second association constant did not converge well or even became close to zero ($K_{\text{NdCl}_2} \sim \mathcal{O}(10^{-7})$).

Based on this observation, the equivalent conductance data obtained below 398 K were modeled with only the first association step $\text{Nd}^{3+} + \text{Cl}^- \rightleftharpoons \text{NdCl}^{2+}$ (Table 3). Figure 7 compares the association constants calculated based on the DEW model^{9,25,28} and empirical correlations by Gammons et al.²⁶

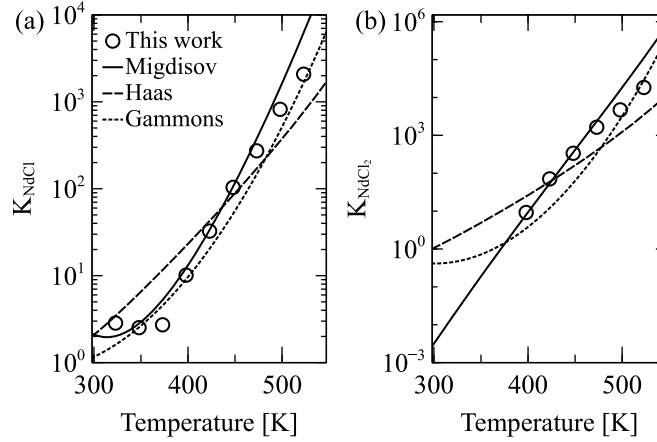


Figure 7: Comparison of association constants obtained from conductance measurements and those from earlier works. Both the first and the second association constants are close to those obtained by Migdisov and Williams-Jones²⁸ and Gammons et al.²⁶

Table 3: Association constants obtained by regressing the TBBK model. At temperatures below 373 K, the second association constants were not calculated because they were statistically insignificant.

T [K]	K_{NdCl}	K_{NdCl_2}
323	2.8 ± 0.0	n/a
348	2.5 ± 0.1	n/a
373	2.7 ± 0.1	n/a
398	10.1 ± 0.5	9.2 ± 0.5
423	32.6 ± 4.9	70.8 ± 22.0
448	103.8 ± 5.3	336.5 ± 156.3
473	273.1 ± 21.6	1641.3 ± 361.7
498	820.2 ± 45.5	4705.7 ± 820.7
523	2079.3 ± 172.7	18358.8 ± 1360.2

Ion speciation results can illustrate the ion pair formation process (Figure 8). At all temperatures, the fraction of the neodymium ions does *not* converge to 100 %, unlike other

neutral cations (e.g., Na^+). This result arises because the ion-pair formation constants between neodymium and hydroxide ions are pretty high, even in room temperature solutions ($K_{\text{NdOH}} \sim \mathcal{O}(10^6)$). The fraction of neodymium hydroxide complexes ($\text{Nd}(\text{OH})_n$), however, rapidly decreases as the concentration of neodymium chloride increases ($c_{\text{Cl}} \gg c_{\text{OH}}$). At the lowest temperature studied in this work (323 K), the fractions of neodymium ion species from different models are similar. At the highest temperature (523 K), the free ion fractions from different association constants are substantially different. The concentration profiles determined in this work are still closer to those calculated based on the DEW parameters provided by Migdisov and Williams-Jones. Hence, this work recommends using the DEW parameters proposed by Migdisov and Williams-Jones when modeling the behavior of neodymium chloride in aqueous solutions (instead of the original parameters by Haas et al.)

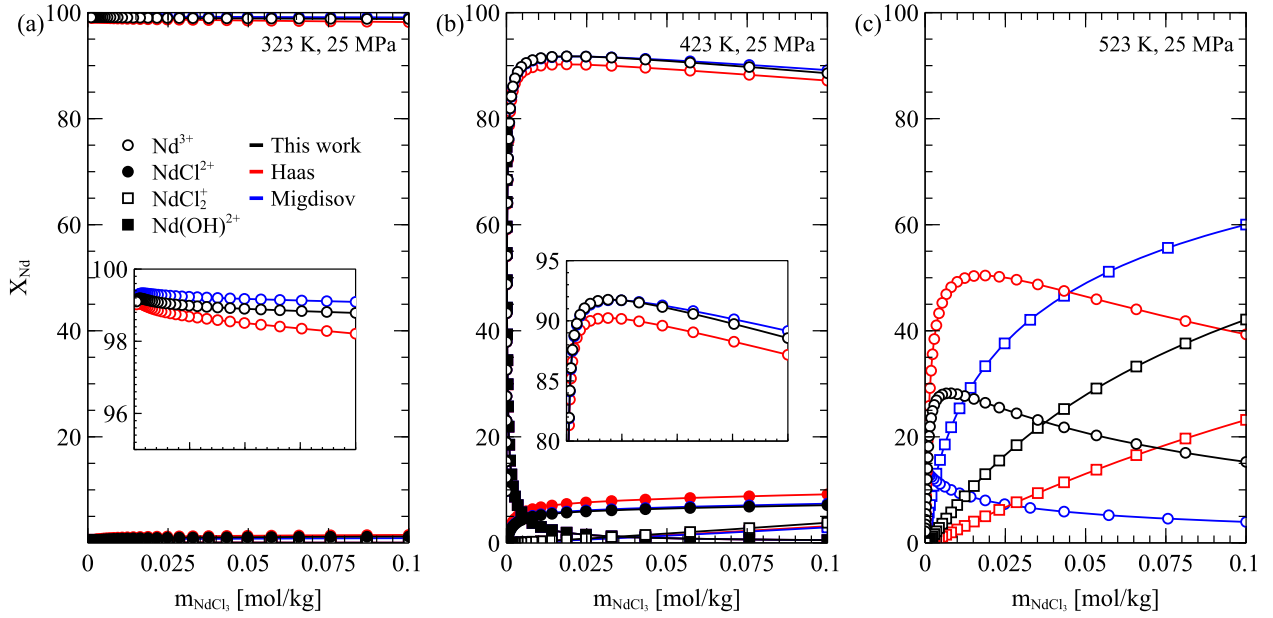


Figure 8: Ion speciation analysis based on different association constants at (a) 323 K, (b) 423 K and (c) 523 K along the 25 MPa isobar. Note that the fraction of free neodymium ions does not converge to 100 %, since the complexation between neodymium and hydroxide ions cannot be ruled out. In all conditions, the concentration profiles from the association constants obtained in this work are closer to those obtained from Migdisov and Williams-Jones. In (a) and (b), insets magnify the difference in the fractions of free neodymium ions. In (c), the fractions of NdCl_2^{2+} and $\text{Nd}(\text{OH})_2^{2+}$ were not shown for visual clarity.

4 Conclusions

In this work, we used the in-situ conductometric device we designed in our earlier work^{12,29,30} to measure complex impedance, from which the limiting conductances and the association constants were estimated in dilute aqueous NdCl_3 solutions up to 523 K along an isobar of 25 MPa. The Turq-Blum-Bernard-Kunz model, which was modified based on several earlier works, was well fitted to the experimental conductance data. The limiting conductances obtained from the model regression agreed well with those calculated from the Smolyakov-Anderko-Lencka correlation, and the association constants were consistent with those obtained by Migdisov and Williams-Jones, and Gammons et al. These consistencies suggest that thermodynamic and kinetic properties (e.g., self-diffusion coefficient of ions in concentrated solutions^{54,55}) can be readily calculated using the modified DEW model parameters and the Smolyakov-Anderko-Lencka correlation. Considering that these thermodynamic and kinetic properties are essential for process design, modeling, and simulations (e.g., in membrane distillation⁷⁰ and precipitation⁷¹), experimental results and derived data reported, as well as the methodology presented in this work can serve as a guide for developing effective and environmentally-friendly REE recovery processes.

Acknowledgement

This work was supported by the Director’s Postdoctoral Fellow Program (20190653PRD4) and the Laboratory Directed Research and Development Program (20190057DR) at Los Alamos National Laboratory.

Supporting Information Available

Corrected expressions for the Turq-Blum-Bernard-Kunz (TBBK) model; Auxiliary equations for speciation analysis; Deep Earth Water (DEW) model parameters and empirical

correlations for calculating association constants; and calculated conductance data based on different models.

Literature Cited

- (1) Liu, H. *Rare Earths: Shades of Grey. Can China Continue To Fuel Our Global Clean & Smart Future*; 2016.
- (2) Xie, F.; Zhang, T. A.; Dreisinger, D.; Doyle, F. A critical review on solvent extraction of rare earths from aqueous solutions. *Minerals Engineering* **2014**, *56*, 10–28.
- (3) Das, G.; Lencka, M. M.; Eslamimanesh, A.; Anderko, A.; Riman, R. E. Rare-earth elements in aqueous chloride systems: Thermodynamic modeling of binary and multicomponent systems in wide concentration ranges. *Fluid Phase Equilibria* **2017**, *452*, 16–57.
- (4) Das, G.; Lencka, M. M.; Eslamimanesh, A.; Wang, P.; Anderko, A.; Riman, R. E.; Navrotsky, A. Rare earth sulfates in aqueous systems: Thermodynamic modeling of binary and multicomponent systems over wide concentration and temperature ranges. *The Journal of Chemical Thermodynamics* **2019**, *131*, 49–79.
- (5) Van Sijl, J.; Allan, N. L.; Davies, G. R.; Van Westrenen, W. Molecular modelling of rare earth element complexation in subduction zone fluids. *Geochimica et Cosmochimica Acta* **2009**, *73*, 3934–3947.
- (6) Finney, A. R.; Lectez, S.; Freeman, C. L.; Harding, J. H.; Stackhouse, S. Ion association in lanthanide chloride solutions. *Chemistry (Weinheim an der Bergstrasse, Germany)* **2019**, *25*, 8725.
- (7) Schijf, J.; Byrne, R. H. Speciation of yttrium and the rare earth elements in seawater: Review of a 20-year analytical journey. *Chemical Geology* **2021**, 120479.

- (8) Cetiner, Z. S.; Wood, S. A.; Gammons, C. H. The aqueous geochemistry of the rare earth elements. Part XIV. The solubility of rare earth element phosphates from 23 to 150 C. *Chemical Geology* **2005**, *217*, 147–169.
- (9) Haas, J. R.; Shock, E. L.; Sassani, D. C. Rare earth elements in hydrothermal systems: estimates of standard partial molal thermodynamic properties of aqueous complexes of the rare earth elements at high pressures and temperatures. *Geochimica et Cosmochimica Acta* **1995**, *59*, 4329–4350.
- (10) Mioduski, T.; Gumiński, C.; Zeng, D. IUPAC-NIST solubility data series. 87. Rare earth metal chlorides in water and aqueous systems. Part 3. Heavy lanthanides (Gd–Lu). *Journal of Physical and Chemical Reference Data* **2009**, *38*, 925–1011.
- (11) Bernard, O.; Kunz, W.; Turq, P.; Blum, L. Conductance in electrolyte solutions using the mean spherical approximation. *The Journal of Physical Chemistry* **1992**, *96*, 3833–3840.
- (12) Yoon, T. J.; Vigil, M. J.; Raby, E. Y.; Singh, R. P.; Maerzke, K. A.; Currier, R. P.; Findikoglu, A. T. Dielectric relaxation of neodymium chloride in water and in methanol. *Journal of Molecular Liquids* **2020**, *308*, 112981.
- (13) Migdisov, A. A.; Reukov, V.; Williams-Jones, A. A spectrophotometric study of neodymium (III) complexation in sulfate solutions at elevated temperatures. *Geochimica et Cosmochimica Acta* **2006**, *70*, 983–992.
- (14) Spedding, F.; Jaffe, S. Conductances, solubilities and ionization constants of some rare earth sulfates in aqueous solutions at 25. *Journal of the American Chemical Society* **1954**, *76*, 882–884.
- (15) Spedding, F.; Yaffe, I. Conductances, transference numbers and activity coefficients of aqueous solutions of some rare earth halides at 25. *Journal of the American Chemical Society* **1952**, *74*, 4751–4755.

- (16) Spedding, F. H.; Rard, J. A.; Saeger, V. W. Electrical conductances of some aqueous rare earth electrolyte solutions at 25. deg.. II. Rare earth chlorides. *Journal of Chemical and Engineering Data* **1974**, *19*, 373–378.
- (17) Apelblat, A. The representation of electrical conductances for polyvalent electrolytes by the Quint-Viallard conductivity equation. Part 3. Unsymmetrical 3: 1, 1: 3, 3: 2, 4: 1, 1: 4, 4: 2, 2: 4, 1: 5 1: 6 and 6: 1 type electrolytes. Dilute aqueous solutions of rare earth salts, various cyanides and other salts. *Journal of solution chemistry* **2011**, *40*, 1291–1316.
- (18) Corti, H. R. In *Hydrothermal Properties of Materials*; Valyashko, V., Ed.; Wiley, 2008; Chapter 4, pp 207–226.
- (19) Ismail, I. M.; Masuko, Y.; Tomiyasu, H.; Fujii, Y. Conductivity of some rare earth chlorides in sub and supercritical aqueous solutions. *The Journal of supercritical fluids* **2003**, *25*, 69–79.
- (20) Helgeson, H. C.; Kirkham, D. H.; Flowers, G. C. Theoretical prediction of the thermodynamic behavior of aqueous electrolytes by high pressures and temperatures; IV, Calculation of activity coefficients, osmotic coefficients, and apparent molal and standard and relative partial molal properties to 600 degrees C and 5kb. *American journal of science* **1981**, *281*, 1249–1516.
- (21) Tanger, J. C.; Helgeson, H. C. Calculation of the thermodynamic and transport properties of aqueous species at high pressures and temperatures; revised equations of state for the standard partial molal properties of ions and electrolytes. *American Journal of Science* **1988**, *288*, 19–98.
- (22) Shock, E. L.; Helgeson, H. C.; Sverjensky, D. A. Calculation of the thermodynamic and transport properties of aqueous species at high pressures and temperatures: Standard

- partial molal properties of inorganic neutral species. *Geochimica et Cosmochimica Acta* **1989**, *53*, 2157–2183.
- (23) Sverjensky, D. A.; Harrison, B.; Azzolini, D. Water in the deep Earth: the dielectric constant and the solubilities of quartz and corundum to 60 kb and 1200 C. *Geochimica et Cosmochimica Acta* **2014**, *129*, 125–145.
- (24) Huang, F.; Sverjensky, D. A. Extended Deep Earth Water Model for predicting major element mantle metasomatism. *Geochimica et Cosmochimica Acta* **2019**, *254*, 192–230.
- (25) Chan, A.; Daswani, M. M.; Vance, S. DEWPython: A Python Implementation of the Deep Earth Water Model and Application to Ocean Worlds. *arXiv preprint arXiv:2105.14096* **2021**,
- (26) Gammons, C.; Wood, S.; Williams-Jones, A. The aqueous geochemistry of the rare earth elements and yttrium: VI. Stability of neodymium chloride complexes from 25 to 300 C. *Geochimica et Cosmochimica Acta* **1996**, *60*, 4615–4630.
- (27) Wood, S. A. The aqueous geochemistry of the rare-earth elements and yttrium: 2. Theoretical predictions of speciation in hydrothermal solutions to 350 C at saturation water vapor pressure. *Chemical Geology* **1990**, *88*, 99–125.
- (28) Migdisov, A. A.; Williams-Jones, A. A spectrophotometric study of neodymium (III) complexation in chloride solutions. *Geochimica et Cosmochimica Acta* **2002**, *66*, 4311–4323.
- (29) Yoon, T. J.; Maerzke, K. A.; Currier, R. P.; Findikoglu, A. T. PyOECF: A flexible open-source software library for estimating and modeling the complex permittivity based on the open-ended coaxial probe (OECF) technique. *arXiv preprint arXiv:2109.14889* **2021**,

- (30) Yoon, T. J.; Riglin, J. D.; Sharan, P.; Currier, R. P.; Maerzke, K. A.; Findikoglu, A. T. An in-situ conductometric apparatus for physicochemical characterization of solutions and in-line monitoring of separation processes at elevated temperatures and pressures. *arXiv preprint arXiv:2109.14884* **2021**,
- (31) Yoon, T. J.; Craddock, E. P.; Lewis, J. C.; Matteson, J. A.; Seong, J. G.; Singh, R. P.; Maerzke, K. A.; Currier, R. P.; Findikoglu, A. T. Selective recovery of critical materials in supercritical water desalination. 2021.
- (32) Velten, D.; Biehl, V.; Aubertin, F.; Valeske, B.; Possart, W.; Breme, J. Preparation of TiO₂ layers on cp-Ti and Ti6Al4V by thermal and anodic oxidation and by sol-gel coating techniques and their characterization. *J. Biomed. Mater. Res.* **2002**, *59*, 18–28.
- (33) Yasensky, D.; Reali, J.; Larson, C.; Carl, C. Citric acid passivation of stainless steel. 2011 Aircraft Airworthiness and Sustainment Conference. 2009.
- (34) Gruszkiewicz, M. S.; Wood, R. H. Conductance of dilute LiCl, NaCl, NaBr, and CsBr solutions in supercritical water using a flow conductance cell. *The Journal of Physical Chemistry B* **1997**, *101*, 6549–6559.
- (35) Quist, A. S.; Marshall, W. L. Electrical conductances of aqueous sodium chloride solutions from 0 to 800. degree. and at pressures to 4000 bars. *The journal of physical chemistry* **1968**, *72*, 684–703.
- (36) Debye, P. The theory of electrolytes I. The lowering of the freezing point and related occurrences. *Physikalische Zeitschrift* **1923**, *24*, 185–206.
- (37) Onsager, L. Zur theorie der elektrolyte (1). *Phys. Z* **1926**, *27*, 28.
- (38) Shedlovsky, T. An equation for electrolytic conductance. *Journal of the American Chemical Society* **1932**, *54*, 1405–1411.

- (39) Fuoss, R. M. Review of the theory of electrolytic conductance. *Journal of Solution Chemistry* **1978**, *7*, 771–782.
- (40) Fernandez-Prini, R. Conductance of electrolyte solutions. A modified expression for its concentration dependence. *Transactions of the Faraday Society* **1969**, *65*, 3311–3313.
- (41) Lee, W. H.; Wheaton, R. J. Conductance of symmetrical, unsymmetrical and mixed electrolytes. Part 1.—Relaxation terms. *Journal of the Chemical Society, Faraday Transactions 2: Molecular and Chemical Physics* **1978**, *74*, 743–766.
- (42) Lee, W. H.; Wheaton, R. J. Conductance of symmetrical, unsymmetrical and mixed electrolytes. Part 2.—Hydrodynamic terms and complete conductance equation. *Journal of the Chemical Society, Faraday Transactions 2: Molecular and Chemical Physics* **1978**, *74*, 1456–1482.
- (43) Lee, W. H.; Wheaton, R. J. Conductance of symmetrical, unsymmetrical and mixed electrolytes. Part 3.—Examination of new model and analysis of data for symmetrical electrolytes. *Journal of the Chemical Society, Faraday Transactions 2: Molecular and Chemical Physics* **1979**, *75*, 1128–1145.
- (44) Quint, J.; Viallard, A. Electrical conductance of electrolyte mixtures of any type. *Journal of Solution Chemistry* **1978**, *7*, 533–548.
- (45) Quint, J.; Viallard, A. The electrophoretic effect for the case of electrolyte mixtures. *Journal of Solution Chemistry* **1978**, *7*, 525–531.
- (46) Quint, J.; Viallard, A. The relaxation field for the general case of electrolyte mixtures. *Journal of Solution Chemistry* **1978**, *7*, 137–153.
- (47) Barthel, J. M.; Krienke, H.; Kunz, W. *Physical chemistry of electrolyte solutions: modern aspects*; Springer Science & Business Media, 1998; Vol. 5.

- (48) Turq, P.; Blum, L.; Bernard, O.; Kunz, W. Conductance in associated electrolytes using the mean spherical approximation. *The Journal of physical chemistry* **1995**, *99*, 822–827.
- (49) Bianchi, H. L.; Dujovne, I.; Fernández-Prini, R. Comparison of electrolytic conductivity theories: performance of classical and new theories. *Journal of solution chemistry* **2000**, *29*, 237–253.
- (50) Sharygin, A. V.; Mokbel, I.; Xiao, C.; Wood, R. H. Tests of equations for the electrical conductance of electrolyte mixtures: measurements of association of NaCl (aq) and Na₂SO₄ (aq) at high temperatures. *The Journal of Physical Chemistry B* **2001**, *105*, 229–237.
- (51) Fernandez, D.; Goodwin, A.; Lemmon, E. W.; Levelt Sengers, J.; Williams, R. A formulation for the static permittivity of water and steam at temperatures from 238 K to 873 K at pressures up to 1200 MPa, including derivatives and Debye–Hückel coefficients. *Journal of Physical and Chemical Reference Data* **1997**, *26*, 1125–1166.
- (52) Huber, M. L.; Perkins, R. A.; Laesecke, A.; Friend, D. G.; Sengers, J. V.; Assael, M. J.; Metaxa, I. N.; Vogel, E.; Mareš, R.; Miyagawa, K. New international formulation for the viscosity of H₂O. *Journal of Physical and Chemical Reference Data* **2009**, *38*, 101–125.
- (53) Wagner, W.; Pruß, A. The IAPWS formulation 1995 for the thermodynamic properties of ordinary water substance for general and scientific use. *Journal of physical and chemical reference data* **2002**, *31*, 387–535.
- (54) Bernard, O.; Kunz, W.; Turq, P.; Blum, L. Self-diffusion in electrolyte solutions using the mean spherical approximation. *The Journal of Physical Chemistry* **1992**, *96*, 398–403.

- (55) Dufrêche, J.-F.; Bernard, O.; Turq, P.; Mukherjee, A.; Bagchi, B. Ionic self-diffusion in concentrated aqueous electrolyte solutions. *Physical review letters* **2002**, *88*, 095902.
- (56) Reilly, P.; Wood, R. H. Prediction of the properties of mixed electrolytes from measurements on common ion mixtures. *The Journal of Physical Chemistry* **1969**, *73*, 4292–4297.
- (57) Wu, Y.; Koch, W.; Zhong, E. C.; Friedman, H. L. The cross-square rule for transport in electrolyte mixtures. *The Journal of Physical Chemistry* **1988**, *92*, 1692–1695.
- (58) Anderko, A.; Lencka, M. M. Computation of electrical conductivity of multicomponent aqueous systems in wide concentration and temperature ranges. *Industrial & engineering chemistry research* **1997**, *36*, 1932–1943.
- (59) Miller, D. G. Binary mixing approximations and relations between specific conductance, molar conductance, equivalent conductance, and ionic conductance for mixtures. *The Journal of Physical Chemistry* **1996**, *100*, 1220–1226.
- (60) Sharygin, A. V.; Grafton, B. K.; Xiao, C.; Wood, R. H.; Balashov, V. N. Dissociation constants and speciation in aqueous Li₂SO₄ and K₂SO₄ from measurements of electrical conductance to 673 K and 29 MPa. *Geochimica et cosmochimica acta* **2006**, *70*, 5169–5182.
- (61) Bandura, A. V.; Lvov, S. N. The ionization constant of water over wide ranges of temperature and density. *Journal of physical and chemical reference data* **2006**, *35*, 15–30.
- (62) Zimmerman, G.; Arcis, H.; Tremaine, P. Limiting conductivities and ion association in aqueous NaCF₃SO₃ and Sr (CF₃SO₃)₂ from (298 to 623) K at 20 MPa. Is triflate a non-complexing anion in high-temperature water? *Journal of Chemical & Engineering Data* **2012**, *57*, 3180–3197.

- (63) Zimmerman, G.; Arcis, H.; Tremaine, P. Limiting conductivities and ion association constants of aqueous NaCl under hydrothermal conditions: experimental data and correlations. *Journal of Chemical & Engineering Data* **2012**, *57*, 2415–2429.
- (64) Marshall, W. L. Reduced state relationship for limiting electrical conductances of aqueous ions over wide ranges of temperature and pressure. *The Journal of chemical physics* **1987**, *87*, 3639–3643.
- (65) Marcus, Y. Ionic radii in aqueous solutions. *Chemical Reviews* **1988**, *88*, 1475–1498.
- (66) Slater, J. C. Atomic radii in crystals. *The Journal of Chemical Physics* **1964**, *41*, 3199–3204.
- (67) Yoon, T. J.; Patel, L. A.; Vigil, M. J.; Maerzke, K. A.; Findikoglu, A. T.; Currier, R. P. Electrical conductivity, ion pairing, and ion self-diffusion in aqueous NaCl solutions at elevated temperatures and pressures. *The Journal of chemical physics* **2019**, *151*, 224504.
- (68) Smolyakov, B.; Veselova, G. Limiting Equivalent Conductivities of Ions in Water Between 25 and 200 C. *Elektrokhim* **1975**, *11*, 700–704.
- (69) Marcus, Y. Viscosity B-coefficients, structural entropies and heat capacities, and the effects of ions on the structure of water. *Journal of Solution Chemistry* **1994**, *23*, 831–848.
- (70) Olatunji, S. O.; Camacho, L. M. Heat and mass transport in modeling membrane distillation configurations: a review. *Frontiers in Energy Research* **2018**, *6*, 130.
- (71) Hodes, M.; Marrone, P. A.; Hong, G. T.; Smith, K. A.; Tester, J. W. Salt precipitation and scale control in supercritical water oxidation—Part A: fundamentals and research. *The Journal of Supercritical Fluids* **2004**, *29*, 265–288.

Graphical TOC Entry

